# Forkhead box protein K1-regulated neurexophilin 4 promotes proliferation, metastasis and glycolysis in colorectal cancer

QIULIN FAN[1*], WAN HE[2*] and YUANJIANG SHANG[3]

[1]Center for Reproductive Medicine; [2]Department of Blood Transfusion; [3]Clinical Laboratory,
Shanghai Tenth People's Hospital, Shanghai 200072, P.R. China

**Abstract.** Colorectal cancer (CRC) is a common malignant tumor. At present, the in-depth study of the formation, development and treatment of CRC at the molecular and gene levels is a research hot spot. Neurexophilin 4 (NXPH4) expression has been revealed to be abnormally elevated in several types of cancer, but its expression in CRC has not yet been reported. First, relevant databases were used to predict the expression of NXPH4 in CRC and its association with the survival rate of patients with CRC. Subsequently, the expression of NXPH4 in CRC cells was verified through cell experiments. Cell Counting Kit-8, 5-ethynyl-2'-deoxyuridine staining, flow cytometry, wound healing assay, Transwell assay, western blotting and the kits were used to detect the effects of NXPH4 knockdown in CRC cells on cell proliferation, invasion, migration and glycolysis. The association between NXPH4 and forkhead box protein K1 (FOXK1) was predicted using the JASPAR database, and verified through luciferase reporter gene and chromatin immunoprecipitation experiments. The NXPH4 regulation mechanism was also discussed. NXPH4 was revealed to be highly expressed in CRC. NXPH4 knockdown in CRC cells could significantly inhibit cell proliferation and induce apoptosis. NXPH4 knockdown inhibited cell invasion, migration and glycolysis. The aforementioned process could be reversed by further FOXK1 overexpression in CRC cells. In conclusion, FOXK1-regulated NXPH4 promotes proliferation, metastasis and glycolysis in CRC.

## Introduction

Colorectal cancer (CRC) is one of the most common malignant tumors worldwide, ranking third in morbidity and second

---

*Correspondence to:* Dr Yuanjiang Shang, Clinical Laboratory, Shanghai Tenth People's Hospital, 301 Yanchang Middle Road, Jing'an, Shanghai 200072, P.R. China
E-mail: shangyuanjiang100@163.com

*Contributed equally

in mortality (1). Approximately 25% of patients with CRC also present with distant metastasis upon initial diagnosis (2). Without treatment, the median survival time of patients with advanced CRC metastasis is 5-6 months (3). With the in-depth study of the formation, development and treatment of CRC at the molecular and genetic levels, targeted therapy with specific selection of binding oncogenic sites has become a research hot spot (4,5). Therefore, it is necessary to explore the pathogenesis of CRC.

Neurexophilin 4 (NXPH4) is a synaptic secretory protein belonging to the NXPH family. Recent studies have revealed that NXPH4 is highly expressed in bladder cancer (6), liver cancer (7), breast cancer (8) and several other types of cancer. A previous study showed that NXPH4 knockdown can inhibit cell proliferation and migration, leading to significant cell cycle stagnation at the S1 stage in non-small cell lung cancer cells (9). However, to the best of our knowledge no studies on NXPH4 in CRC have been reported so far.

Therefore, the aim of the present study was to preliminarily explore the occurrence and development mechanism of CRC by studying the mechanism of NXPH4 in CRC. We hope that the present study can provide a theoretical basis for the clinical targeted treatment of CRC.

## Materials and methods

*Databases.* The ENCORI database predicted the expression of NXPH4 in patients with CRC (10). The ENCORI database predicted the association between high NXPH4 expression and overall survival in patients with CRC (the median 50% value was used as the cutoff for high and low) (11). The JASPAR database predicted the binding sites of transcription factor forkhead box protein K1 (FOXK1) and NXPH4 promoter (12).

*Cell culture.* The Caco2, LoVo, SW480 and HCT116 cells and HIEC normal intestinal epithelial cell lines were obtained from the American Type Culture Collection and cultured at 37˚C in a 5% $CO_2$ with DMEM (Gibco; Thermo Fisher Scientific, Inc.) supplemented with 10% FBS (Gibco; Thermo Fisher Scientific, Inc.).

*Reverse transcription-quantitative PCR (RT-qPCR).* Total RNA was extracted using TRIzol® reagent (Thermo Fisher

Scientific, Inc.). RNA concentration was quantified by spectrophotometry (GeneQuant; GE Healthcare) at 260 nm. Next, cDNA was produced by RT using SuperScript™ IV VILO™ Master Mix (Thermo Fisher Scientific, Inc.) at 37°C for 60 min and then at 95°C for 5 min. The miScript HiSpec Buffer (Qiagen AB) and ABI 7500 real-time PCR system (Applied Biosystems; Thermo Fisher Scientific, Inc.) were used for qPCR. The PCR program began with an initial denaturation at 95°C for 2 min, followed by 40 amplification reaction cycles (95°C for 30 sec, 55°C for 30 sec and 72°C for 30 sec), with a final extension at 72°C for 3 min. The data were processed using the $2^{-\Delta\Delta Cq}$ method (13). GAPDH was used as an endogenous control. NXPH4 forward, 5'-TGTCGAGTT CGGAGGAGTCT-3' and reverse, 5'-GCTATCCGAAGTAGG GGTGC-3'; FOXK1 forward, 5'-GCGCATTCTTCCTGTTAG CG-3' and reverse, 5'-GGCTACCGGTTCCAAGACAA-3'; and GAPDH forward, 5'-CATGAGAAGTATGACAACAGC CT-3' and reverse, 5'-AGTCCTTCCACGATACCAAAGT-3'.

*Western blotting.* Cells were lysed with RIPA Lysis Buffer (Thermo Fisher Scientific, Inc.). A Pierce BCA protein assay kit was used to measure protein concentration (Thermo Fisher Scientific, Inc.). A total of 30 µg protein (per lane) was separated using 10% SDS-PAGE and transferred onto a PVDF membrane (Merck KGaA). After blocking the membranes with 5% bovine serum albumin (Applygen Technologies, Inc.) at room temperature for 1.5 h, the protein bands were incubated overnight at 4°C with the primary antibodies NXPH4 (cat. no. ab74999), E-cadherin (cat. no. ab40772), N-cadherin (cat. no. ab76011), Vimentin (cat. no. ab92547), glucose transporter 1 (GLUT1; cat. no. ab115730), hexokinase 2 (HK2; cat. no. ab209847), pyruvate kinase isozymes M1/M2 (PKM2; cat. no. ab85555), FOXK1 (cat. no. ab309510), and GAPDH (cat. no. ab9485) (all 1:1,000; Abcam) On the second day, the secondary antibodies were incubated for 1 h at room temperature and the membranes were then developed with Clarity Western ECL substrate (Bio-Rad Laboratories, Inc.), visualized with a ChemiDoc™ MP Imaging System (Bio-Rad Laboratories, Inc.) and analyzed using Quantity One 4.62 analysis software (Bio-Rad Laboratories, Inc.).

*Cell transfection.* The expression of NXPH4 was knocked down by short hairpin (sh)RNAs (sh-NXPH4#1 and sh-NXPH4#2) constructed in lentiviral plasmids (pCLenti-U6-shRNA-CM V-EGFP-WPRE) using a 2nd generation system. The Trpv1 pGHH1 plasmid and scrambled control shRNA (sh-NC; 2 µg) were synthesized by OBiO Technology (Shanghai) Corp., Ltd. HCT116 cells were transducted with the lentivirus at a multiplicity of infection of 1 using 50 nM Lipofectamine® 2000 transfection reagent, according to the manufacturer's instructions. Cells were transfected with the pcDNA3.1 vector (GeneChem, Inc.) containing full-length FOXK1 (Oe-FOXK1; 2 µg) and control (Oe-NC; 2 µg) plasmids at 37°C for 48 h using Lipofectamine 2000 transfection reagent, according to the manufacturer's instructions. At 24 h after transfection, cells were selected with puromycin (5 µg/ml) for 2 days and maintained with 0.25 µg/ml puromycin. After 48 h, RT-qPCR and western blotting were performed to detect the transfection efficiency. The target sequence of sh-NXPH4#1 is 5'-AGA GTCACGCGCTTTCAATTG-3' and sh-NXPH4#2 is 5'-AGA

AGGTGTGCCCAGACTATA-3'; shRNA-NC, 5'-CAACAA GATGAAGAGCACCAA-3'

*Cell Counting Kit (CCK)-8 assay.* Transfected cell suspensions were seeded on 96-well plates at a density of 1,500 cells/well for 24, 48 and 72 h. Next, 10 µl CCK-8 solution (MedChemExpress) was added to each well. After 2 h of incubation, a microplate analyzer was used to read the absorbance of each well at 450 nm.

*5-Ethynyl-2'-deoxyuridine (EdU) incorporation assay.* HCT116 cells were seeded onto 96-well plates at a density of $5x10^3$ per well. The cells were incubated for an additional 2 h in medium containing 50 µM EdU (Guangzhou RiboBio Co., Ltd.). Cells were then fixed and permeabilized with PBS containing 4% paraformaldehyde for 15 min at room temperature and 0.5% Triton X-100 at room temperature for 10 min, followed by incubation with 1x Apollo reaction cocktail (100 µl/well) for 30 min at room temperature. DNA was incubated with 4',6-diamidino-2-phenylindole stain (100 µl/well) for 30 min at room temperature and visualized using an inverted fluorescence microscope (Leica). Captured images were processed and analyzed with ImageJ software (version 1.8.0; National Institutes of Health).

*Apoptosis assay.* Apoptosis was detected using an annexin V-fluorescein isothiocyanate (FITC)/propidium iodide (PI) apoptosis detection kit (Sangon Biotech Co., Ltd.), according to the manufacturer's instructions. In brief, HCT116 cells were harvested, incubated with Annexin V-FITC for 15 min at room temperature and re-stained with PI in the dark for 15 min at room temperature. Apoptotic cells were measured using a flow cytometer (BD Biosciences) and analyzed with FlowJo software (version X; FlowJo LLC).

*Cell migration and invasion assays.* HCT116 cells ($6x10^4$ cells) were plated in the upper chambers that had been coated with Matrigel (BD Biosciences) for 1 h at 37°C to estimate tumor invasion, and the upper chambers without Matrigel were used to assess tumor cell migration, respectively. For cell invasion, the Transwell inserts (8-µm pore-size; Corning, Inc.) were put into 24-well plates. Cells ($5x10^4$) in serum-free DMEM were seeded into the upper chambers while the lower chambers were filled with DMEM with 10% FBS. After 24 h at 37°C, the upper chambers with the residual cells were removed and the cells under the surface were stained with 0.5% crystal violet for 10 min at room temperature and then fixed with 70% ethanol for 30 min at room temperature. Cells were counted with an inverted light microscope (Olympus) using ImageJ software (version 1.8.0; National Institutes of Health).

For cell migration, HCT116 cells were seeded in six-well plates at the density of $5x10^5$ cells/well. When the cells were grown to 90-100% confluence, artificial wounds were gently made using a micropipette tip, and confluent monolayers for wounding were yielded. The original culture medium was replaced with serum-free DMEM supplemented with 30 µg/ml mitomycin. Cells in the scratched area were imaged at 0 and 24 h using a light microscope. The relative migrating distance was the ratio of migration distance at 24 h and the distance measured at 0 h.

*Oxygen consumption rate (OCR) and extracellular acidification rate (ECAR) detection.* Cellular ECAR and OCR were measured with a Seahorse Bioscience XF96 Extracellular Flux Analyzer. In brief, $2x10^4$ cells were seeded into 96-well cell culture XF microplates and incubated overnight at 37°C for further testing, according to the manufacturer's instructions. The ECAR and OCR values were calculated after normalization to the total cell number.

*Glucose uptake and lactate product assay.* The relative glucose uptake was assessed by measuring the glucose concentration in the medium using Glucose Assay kit (cat. no. CBA086; Merck KGaA), and the lactate production in the medium was detected using a Lactate Assay kit (cat. no. BC2235), according to the manufacturer's instructions (Beijing Solarbio Science & Technology Co., Ltd).

*Dual-luciferase reporter assay.* Luciferase assays were performed using 96-well plates. The site of NXPH4 binding of FOXK1 that mutated (MUT-NXPH4) and the site of wild-type NXPH4 (WT-NXPH4) were amplified by RT-qPCR and cloned into the pMIR-REPORT™ vector (Ambion; Thermo Fisher Scientific, Inc.). The constructs Oe-FOXK1 and Oe-NC were co-transfected into cells with Lipofectamine 2000. Following 48 h of plasmid co-transfection, the luciferase signals were measured using 50 μl Stop&Glo Reagent, according to the manufacturer's instructions [OBiO Technology (Shanghai) Corp., Ltd.]. The *Renilla* luciferase levels were normalized to firefly luciferase levels.

*Chromatin immunoprecipitation assay (ChIP).* ChIP assays were performed with a EZ-Magna ChIP kit (cat. no. 17-408; Merck KGaA), according to the manufacturer's instructions. In brief, the cells were lysed in SDS Lysis Buffer in an ice bath for 10 min. After sonicating the samples (20 kHz; 4 pulses of 12 sec each, followed by 30 sec rest on ice between each pulse), 1.8 ml ChIP dilution buffer was added. Subsequently, 50 μg protein-A-agarose was added for 30 min at 4°C. After centrifugation at 1,000 x g for 3 min at 4°C, the supernatant (100 μg) was removed and incubated with 3 μg indicated antibody FOXK1 (1:200; cat. no. ab309510; Abcam) and 50 μg protein-A-agarose overnight at 4°C. Isotype-matched IgG (1:100; cat. no. ab172730; Abcam) was used as the negative control. The precipitate was collected after incubating at 4°C for 6 h and centrifugated at 1,000 x g at 4°C for 3 min. Following washing, chromatin from beads was eluted with gentle vortexing (1,200 rpm) at 65°C for 30 min. The DNA was then purified using an RT-qPCR Purification Kit (Qiagen AB).

*Statistical analysis.* Statistical analysis was performed using GraphPad Prism 5.0 (GraphPad Software, Inc.). All data are expressed as the mean ± SD (unless otherwise shown). Multiple group comparisons were performed using ANOVA followed by Tukey's post-hoc test. $P<0.05$ was considered to indicate a statistically significant difference. The $\chi^2$ test and unpaired Student's t-test were used to examine the connection between NXPH4 expression and clinical features. All experiments were repeated independently three times.

Table I. Association of NXPH4 expression and clinicopathological parameters in patients with colorectal cancer.

| Characteristics | NXPH4 expression in the TCGA database | | P-value |
| --- | --- | --- | --- |
| | Low (n=296) | High (n=294) | |
| Sex, n (%) | | | 0.218 |
| Female | 132 (22.4) | 147 (24.9) | |
| Male | 164 (27.8) | 147 (24.9) | |
| Age, n (%) | | | 0.264 |
| ≤60 | 87 (14.7) | 100 (16.9) | |
| >60 | 209 (35.4) | 194 (32.9) | |
| Age, median (IQR) | 67 (59-76) | 66 (56-76) | 0.428 |

NXPH4, neurexophilin 4; IQR, interquartile range.

## Results

*NXPH4 is highly expressed in CRC.* The ENCORI database predicted a high expression of NXPH4 in patients with CRC compared with control patients, and higher NXPH4 expression was strongly associated with tumor stages and nodal metastasis status (Fig. 1A). The Kaplan-Meier Plotter database predicted that high NXPH4 expression was significantly associated with low overall survival in patients with CRC (Fig. 1B). Clinical data on 590 patients with CRC were gathered from the TCGA database for the present investigation (Table I). According to the median mRNA expression levels of NXPH4, patients with CRC were split into low and high expression groups. The relationship between NXPH4 expression and several clinical features of patients with CRC such as age and sex were investigated. It was revealed that there was no association between high NXPH4 mRNA expression and age and sex ($P>0.05$). RT-qPCR and western blotting for NXPH4 expression in CRC cells showed that, as compared with HIEC cells, NXPH4 expression in CRC cell lines was significantly increased (Fig. 1C). Among them, the increase in HCT116 cells was the most significant, so the HCT116 cell line was selected for follow-up experiments.

*NXPH4 interference inhibits CRC cell proliferation and induces their apoptosis.* NXPH4 expression in HCT116 cells was then knocked down, and transfection efficacy was detected using RT-qPCR and western blotting. It was discovered that NXPH4 expression was prominently decreased following transfection of sh-NXPH4#1/2 (Fig. 2A). sh-NXPH4#2 was selected for follow-up experiments, and cells were divided into the control, sh-NC and sh-NXPH4 groups. CCK-8 and EdU staining were used to detect cell viability and proliferation. The results showed that, as compared with the sh-NC group, cell viability in the sh-NXPH4 group was significantly decreased at 48 and 72 h, as was cell proliferation (Fig. 2B and C). Flow cytometry showed that NXPH4 overexpression significantly increased apoptosis compared with sh-NC (Fig. 2D).

*NXPH4 interference inhibits CRC metastasis and glycolysis.* Wound healing and Transwell assays were performed to
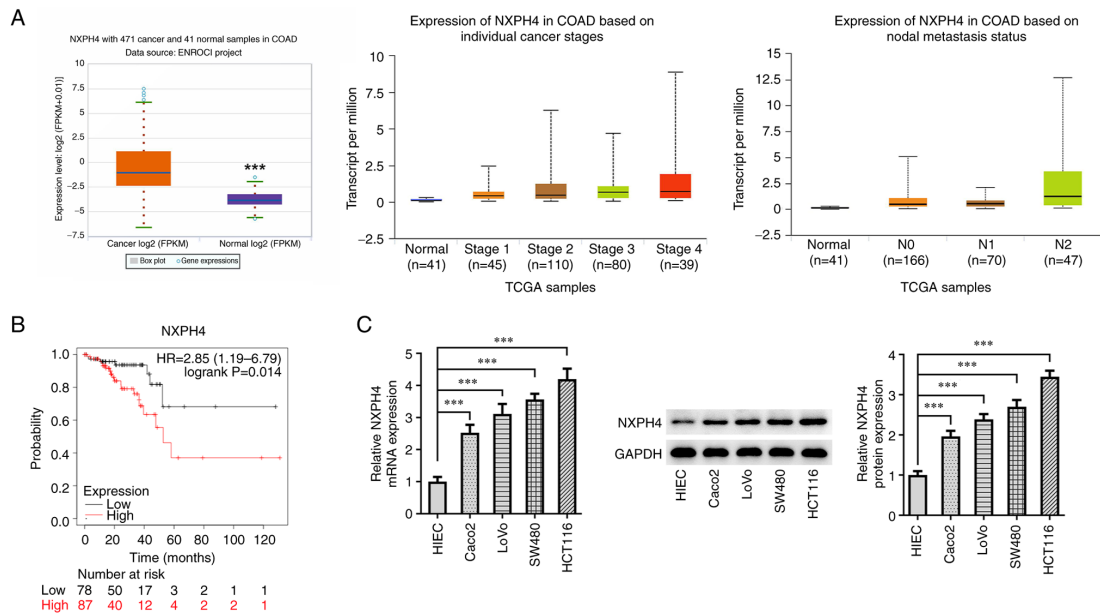
Figure 1. NXPH4 is highly expressed in colorectal cancer. (A) ENCORI database predicted the high NXPH4 expression in patients with CRC, and the association of NXPH4 expression with tumor stages and nodal metastasis status. (B) Kaplan-Meier Plotter database predicted that high NXPH4 expression was significantly associated with low overall survival in patients with CRC. (C) Reverse transcription-quantitative PCR and western blotting were used to detect NXPH4 expression in CRC cells. ***$P<0.001$. COAD, colon adenocarcinoma; NXPH4, neurexophilin 4; CRC, colorectal cancer.
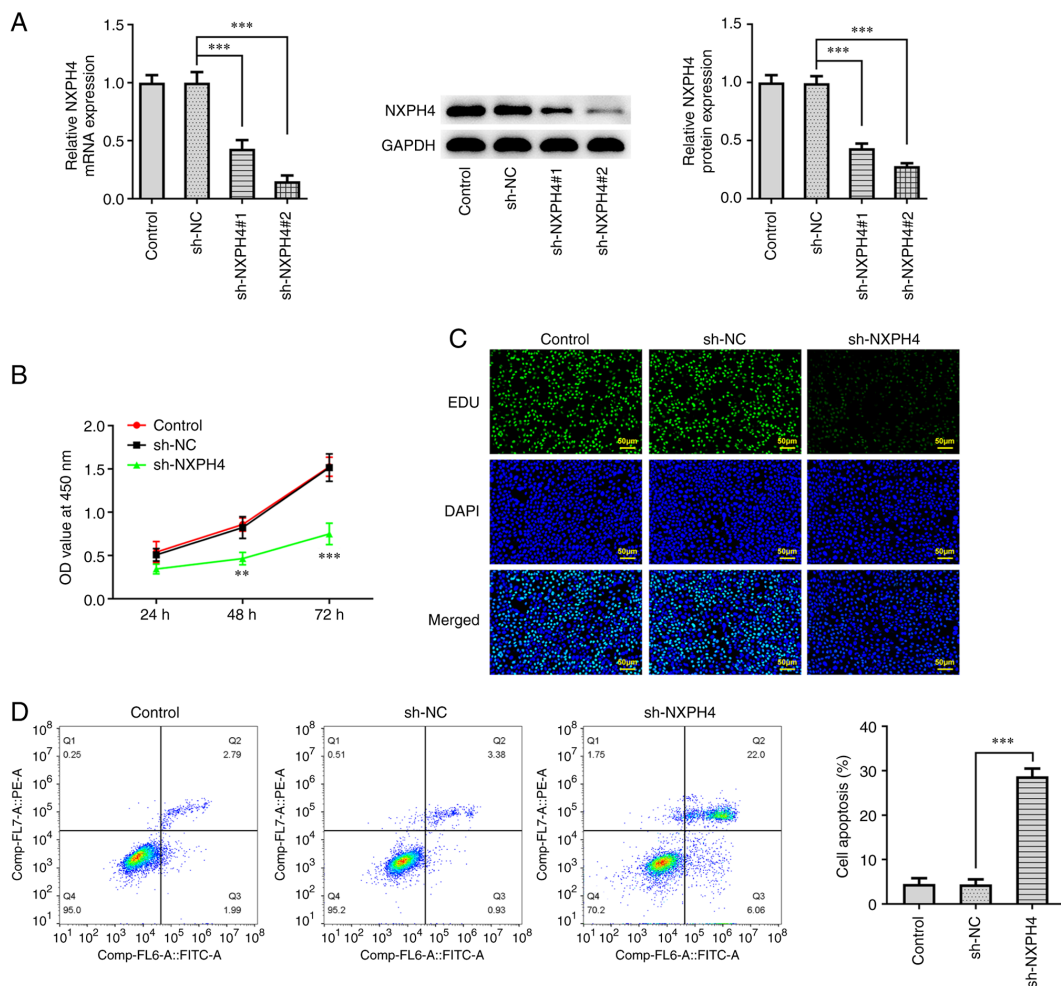


Figure 2. NXPH4 interference inhibits the proliferation and induces apoptosis of CRC cells. (A) NXPH4 expression in HCT116 cells was then knocked down, and transfection efficacy was detected by reverse transcription-quantitative PCR and western blotting. (B) Cell-Counting Kit-8 assay and (C) EdU staining were used to detect cell viability and proliferation. (D) Flow cytometry was used to detect cell apoptosis. **$P<0.01$ and ***$P<0.001$ compared with sh-NC. NXPH4, neurexophilin 4; CRC, colorectal cancer; EdU, 5-ethynyl-2'-deoxyuridine; sh, short hairpin; NC, negative control.
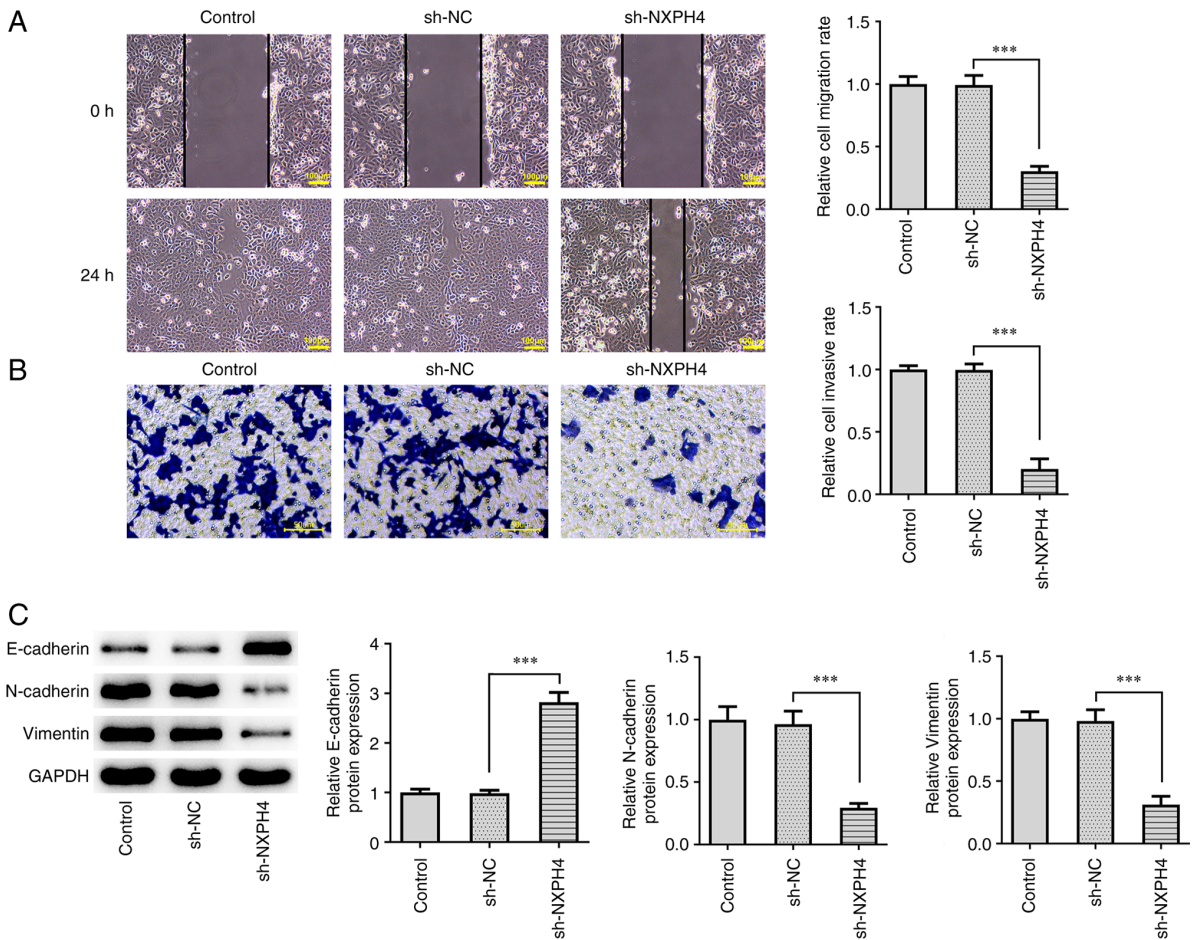
Figure 3. NXPH4 interference inhibits metastasis of CRC cells. (A) Wound healing (scale bar, 100 $\mu$m) and (B) Transwell assays (scale bar, 50 $\mu$m) were performed to determine cell migration and invasion. (C) Western blotting was used to detect EMT-related proteins. ***P<0.001. NXPH4, neurexophilin 4; CRC, colorectal cancer; EMT, epithelial-mesenchymal transition; sh, short hairpin; NC, negative control.
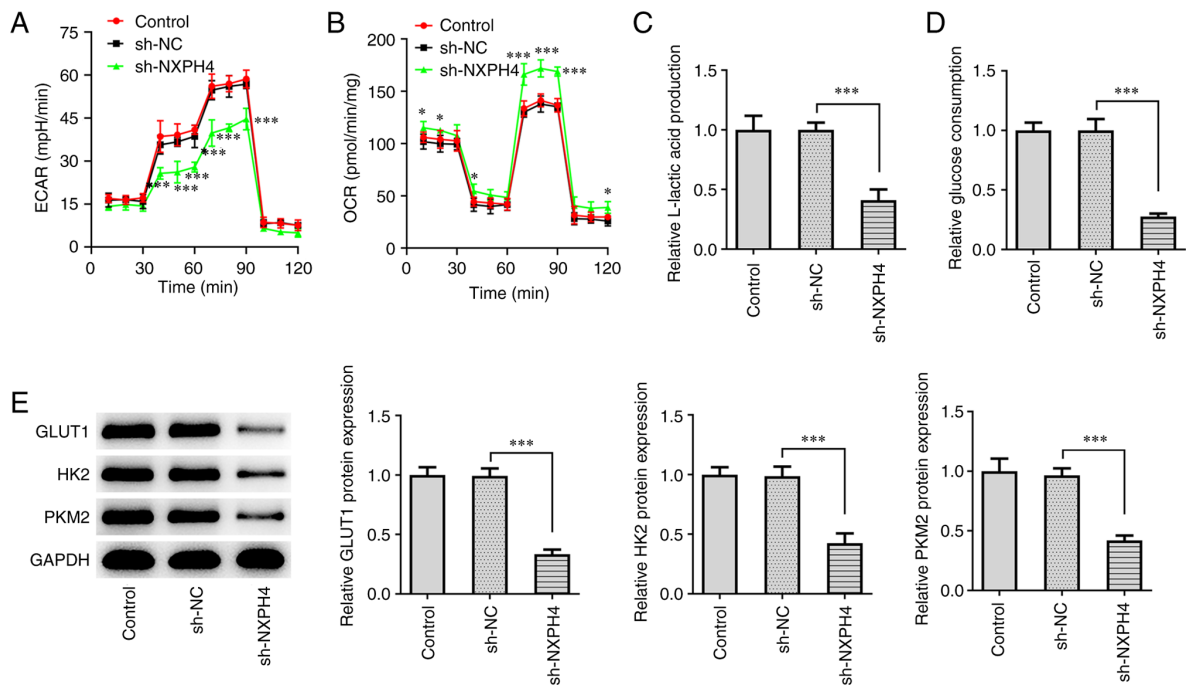


Figure 4. NXPH4 interference inhibits glycolysis of CRC cells. XF96 extracellular flux analyzer detected (A) ECAR and (B) OCR. Glucose uptake and lactate product assay were used to detect (C) lactic acid production and (D) glucose consumption. (E) Western blotting was used to detect GLUT1, HK2 and PKM2 protein expression. *P<0.05 and ***P<0.001. NXPH4, neurexophilin 4; CRC, colorectal cancer; ECAR, extracellular acidification rate; OCR, oxygen consumption rate; GLUT1, glucose transporter 1; HK2, hexokinase 2; PKM2, pyruvate kinase isozymes M1/M2; sh, short hairpin; NC, negative control.
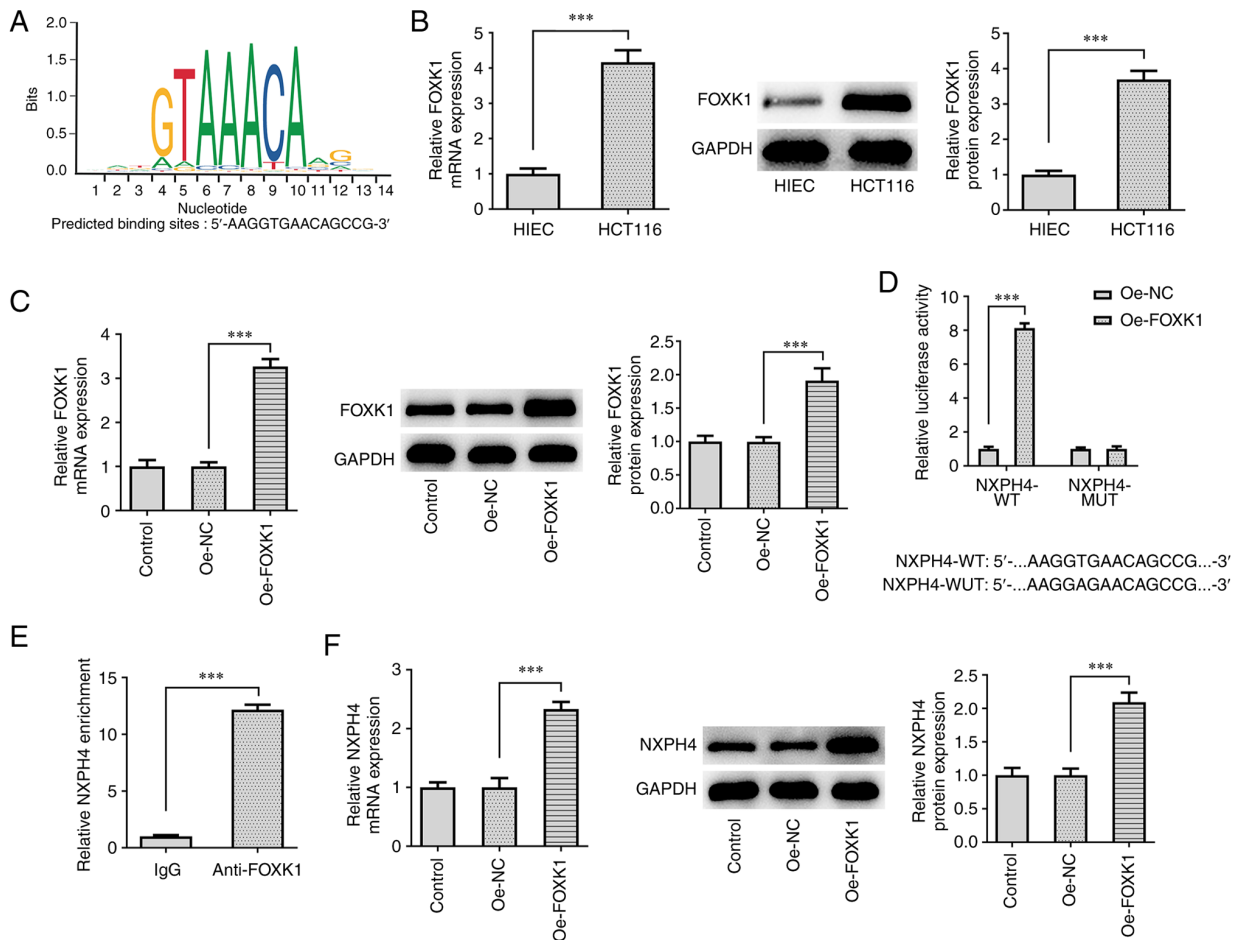
Figure 5. FOXK1 promotes NXPH4 transcription. (A) JASPAR database predicted that the transcription factor FOXK1 and NXPH4 promoter had binding sites. (B) RT-qPCR and western blotting were used to detect FOXK1 expression in CRC cells. (C) FOXK1 overexpression plasmid was constructed, and transfection efficacy was detected by RT-qPCR and western blotting. (D) Luciferase and (E) ChIP experiments confirmed the binding relationship between NXPH4 and FOXK1. (F) Following FOXK1 overexpression, RT-qPCR and western blotting were performed to detect the expression of NXPH4 to test its effect. ***P<0.001. FOXK1, forkhead box protein K1; NXPH4, neurexophilin 4; RT-qPCR, reverse transcription-quantitative PCR; CRC, colorectal cancer; ChIP, chromatin immunoprecipitation assay; sh, short hairpin; NC, negative control; WT, wild-type; MUT, mutant.
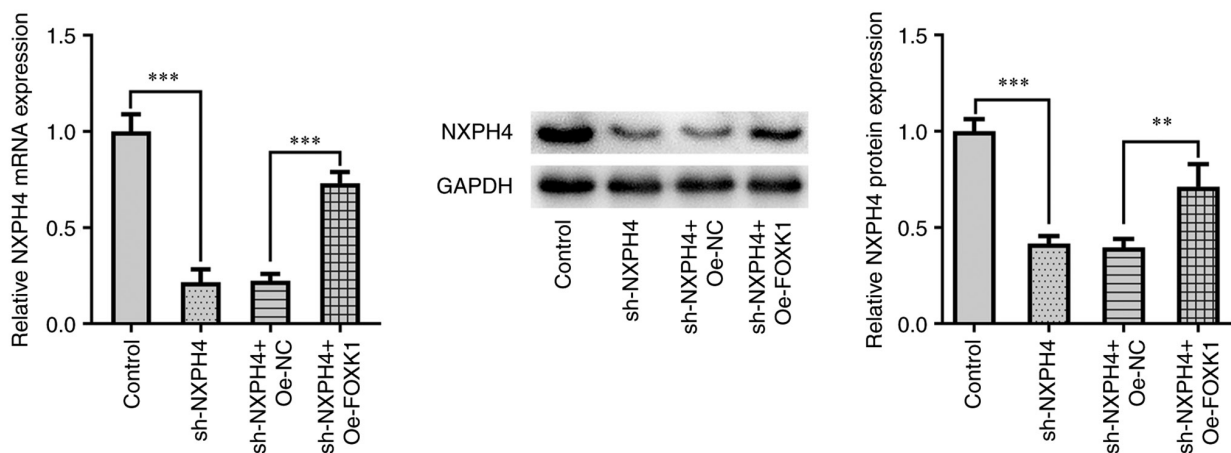


Figure 6. Transfection efficiency of cells. The expression of NXPH4 was detected by western blot after cell transfection. **P<0.01 and ***P<0.001. FOXK1, forkhead box protein K1; NXPH4, neurexophilin 4; sh, short hairpin; NC, negative control; Oe, overexpression.

evaluate cell migration and invasion. The results showed that, following NXPH4 interference, the invasion and migration ability of cells were significantly decreased compared with the sh-NC group (Fig. 3A and B). Western blotting

examined the expression of epithelial-mesenchymal transition (EMT)-related proteins and the results indicated that NXPH4 interference elevated E-cadherin expression, whereas it decreased N-cadherin and Vimentin expression (Fig. 3C).
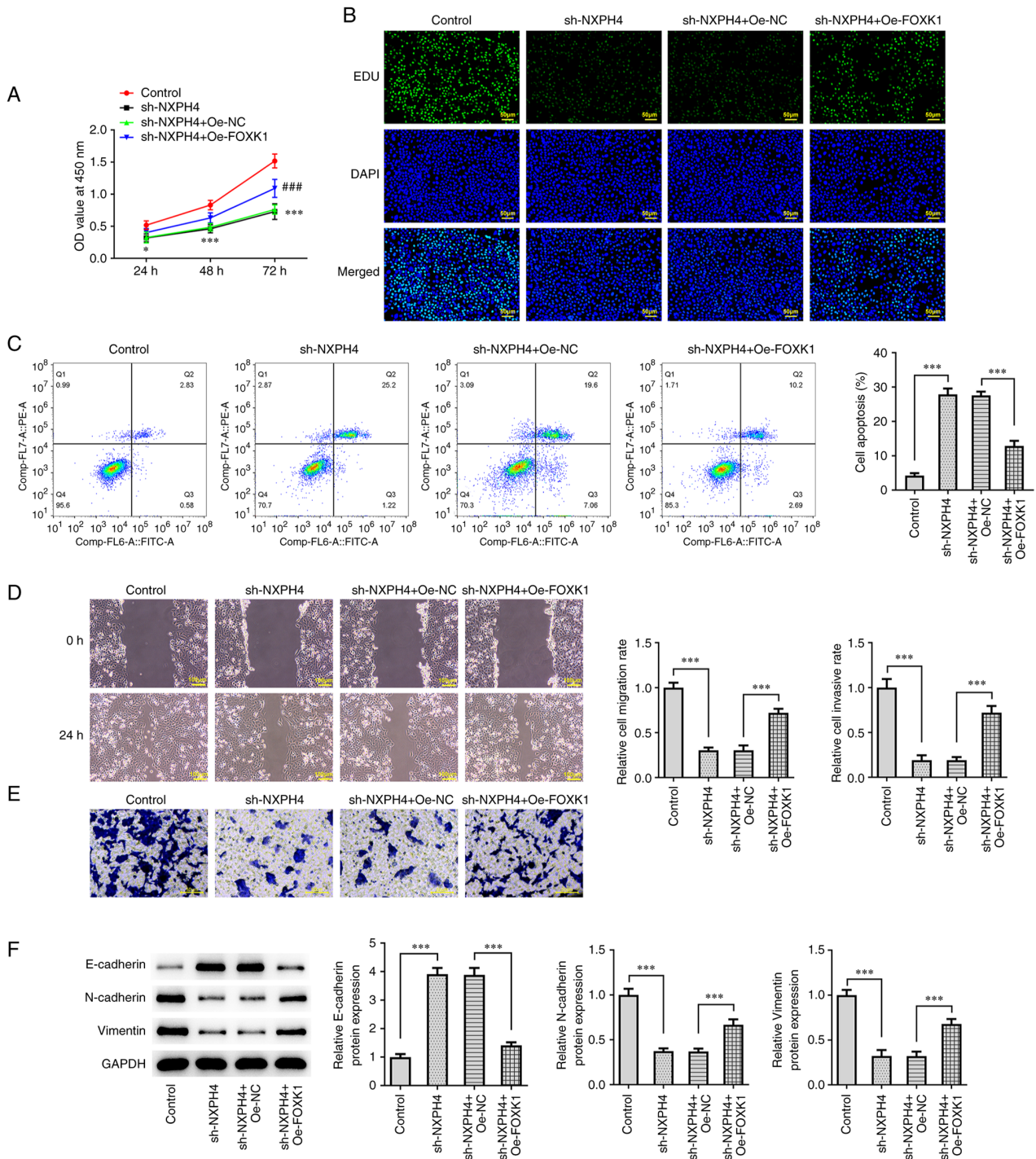
Figure 7. Overexpression of FOXK1 reverses the effect of NXPH4 interference on CRC cells. (A) Cell-Counting Kit-8 assay and (B) EdU staining were performed to detect cell viability and proliferation (scale bar, 50 $\mu$m). (C) Flow cytometry was performed to detect apoptosis. (D) Wound healing (scale bar, 100 $\mu$m) and (E) Transwell assays (scale bar, 50 $\mu$m) were performed for cell migration and invasion. (F) Western blotting was used to detect epithelial-mesenchymal transition-related proteins. *P<0.05, ***P<0.001 and ###P<0.001 vs sh.NXPH4 + Oe-NC. FOXK1, forkhead box protein K1; NXPH4, neurexophilin 4; CRC, colorectal cancer; EdU, 5-ethynyl-2'-deoxyuridine; sh, short hairpin; NC, negative control; Oe, overexpression.

XF96 extracellular flux analyzer detected ECAR and OCR, and the results showed that, as compared with sh-NC, ECAR was significantly decreased and OCR was significantly increased in the sh-NXPH4 group (Fig. 4A and B). The results of glucose uptake and lactate product assay revealed a significant decrease in lactic acid production and glucose consumption in the sh-NXPH4 group, as compared with the sh-NC group (Fig. 4C and D). Western blotting for glucose

uptake-related protein expression showed that GLUT1, HK2 and PKM2 expression was significantly decreased following NXPH4 interference (Fig. 4E). The aforementioned results showed that NXPH4 interference inhibited CRC metastasis and glycolysis.

*FOXK1 promotes NXPH4 transcription.* The JASPAR database predicted that the transcription factor FOXK1 and NXPH4
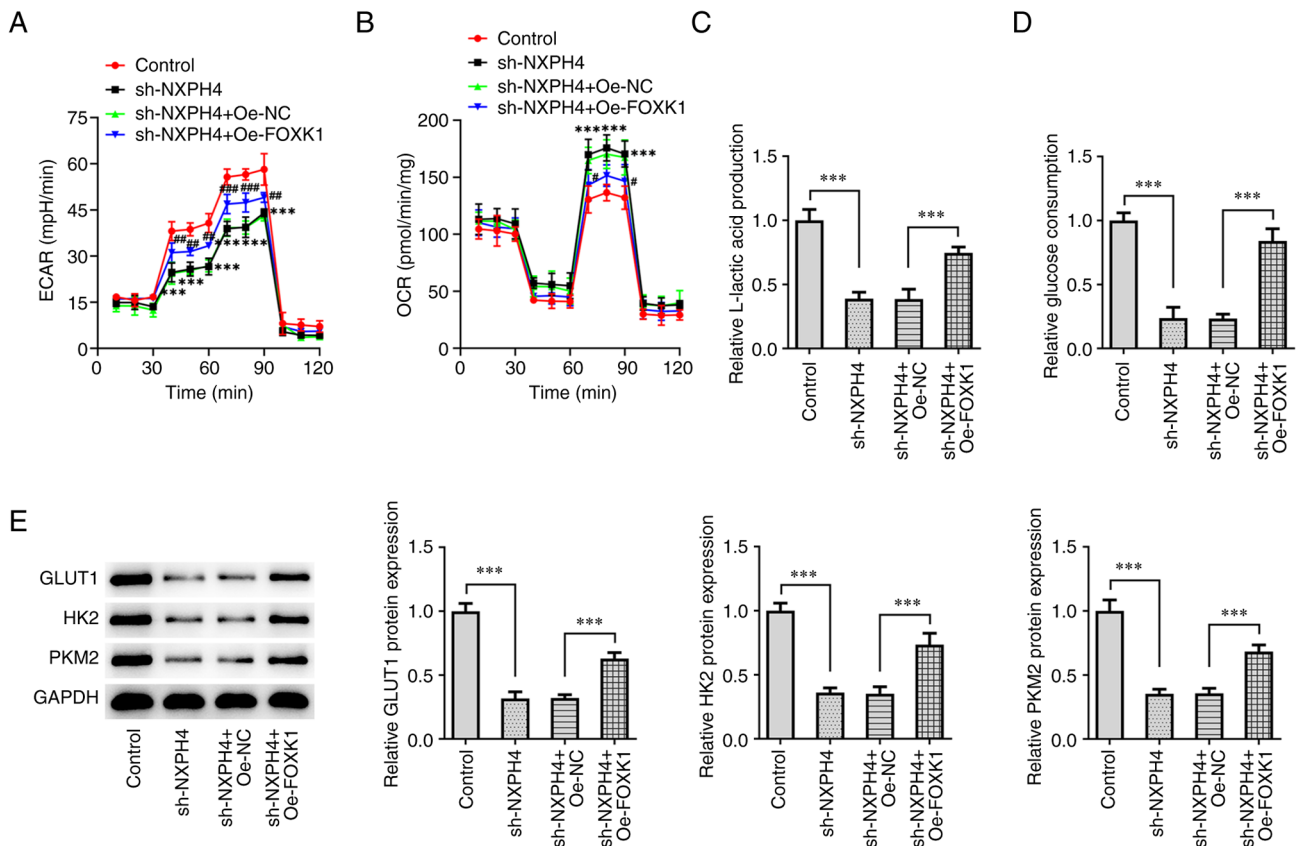
Figure 8. FOXK1 overexpression reverses the effect of NXPH4 interference on CRC cells. XF96 extracellular flux analyzer detected (A) ECAR and (B) OCR. ***P<0.001 compared with Control; #P<0.05, ##P<0.01 and ###P<0.001 compared with sh-NXPH4 + Oe-NC. Glucose uptake and lactate product assay were performed to detect (C) lactic acid production and (D) glucose consumption. (E) Western blotting was performed to detect GLUT1, HK2 and PKM2 proteins. ***P<0.001. FOXK1, forkhead box protein K1; NXPH4, neurexophilin 4; CRC, colorectal cancer; ECAR, extracellular acidification rate; OCR, oxygen consumption rate; GLUT1, glucose transporter 1; HK2, hexokinase 2; PKM2, pyruvate kinase isozymes M1/M2; sh, short hairpin; NC, negative control; Oe, overexpression.

promoter had binding sites (Fig. 5A). RT-qPCR and western blotting results showed that FOXK1 expression was significantly increased in CRC cells compared with HIEC cells (Fig. 5B). FOXK1 overexpression plasmid was constructed, and transfection efficacy was detected by RT-qPCR and western blotting. FOXK1 expression was increased following transfection of Oe-FOXK1 (Fig. 5C). Luciferase reporter assay demonstrated that FOXK1 overexpression markedly enhanced the luciferase activity of NXPH4-WT but not NXPH4-MUT (Fig. 5D). ChIP experiments confirmed that NXPH4 promoter was abundant in FOXK1 antibody (Fig. 5E), implying the binding relationship between NXPH4 and FOXK1. Subsequently, following FOXK1 overexpression, RT-qPCR and western blotting were used to detect the expression of NXPH4 to test its effect, and NXPH4 expression was discovered to be increasing when FOXK1 was overexpressed (Fig. 5F).

*Overexpression of FOXK1 reverses the effect of NXPH4 interference on CRC cells.* Cells were grouped into the control, sh-NXPH4, sh-NXPH4 + Oe-NC and sh-NXPH4 + Oe-FOXK1 groups. The expression of NXPH4 was detected by RT-qPCR and western blotting, and it was noted that the depleted NXPH4 expression level due to knockdown of NXPH4 was markedly increased after overexpression of FOXK1 (Fig 6). CCK-8 and EdU staining results showed that

cell viability and proliferation were significantly increased in sh-NXPH4 + Oe-FOXK1, as compared with sh-NXPH4 + Oe-NC group (Fig. 7A and B). Flow cytometry showed that the apoptosis in the sh-NXPH4 + Oe-FOXK1 group was significantly decreased compared with that in the sh-NXPH4 + Oe-NC group (Fig. 7C). Cell migration and apoptosis results showed that cell migration and invasion were significantly increased in the sh-NXPH4 + Oe-FOXK1 group, as compared with the sh-NXPH4 + Oe-NC group (Fig. 7D and E). Western blotting results of EMT markers showed that FOXK1 overexpression could significantly reverse the effect of NXPH4 interference on EMT-related proteins (Fig. 7F). Next, glycolysis-related indicators were detected, and the results showed that, as compared with the sh-NXPH4 + Oe-NC group, the sh-NXPH4 + Oe-FOXK1 group exhibited increased ECAR, decreased OCR, increased lactate level, increased glucose consumption and increased expression of glycolysis-related proteins GLUT1, HK2 and PKM2 (Fig. 8A-E).

## Discussion

CRC can seriously harm human health and has a high incidence and rate of mortality (14). Traditional treatments for CRC include surgical therapy and chemoradiotherapy. Currently, the rise of molecular targeted therapy and immunotherapy

has provided new prospects for the treatment of CRC, but the prognosis of patients with advanced CRC remains poor. In addition, traditional tumor markers, such as carcinoembryonic antigen and carbohydrate antigen 199, have poor sensitivity and specificity in predicting the occurrence of CRC (15). In recent years, an increasing number of studies have focused on finding new and more sensitive tumor markers for the diagnosis and treatment of CRC (16,17).

NXPH4 can be used as a biomarker for the early diagnosis of hepatocellular carcinoma (18). The upregulation of NXPH4 is associated with the poor prognosis of hepatocyte carcinoma and immune cell invasion. NXPH4 knockdown significantly inhibits the proliferation, migration and invasion of JHH7 and SNU182 cells (7). In addition, NXPH4 promotes the proliferation, migration and invasion of bladder cancer cells by maintaining the stability of NDUFA4 mitochondrial complex associated-like-2, thereby activating reactive oxygen species and glycolysis (19). Using relevant websites, the present study predicted that NXPH4 expression was significantly increased in patients with CRC, and that high NXPH4 expression was significantly associated with a lower overall survival in patients with CRC. Therefore, the current study speculated that NXPH4 also plays a regulatory role in CRC. Therefore, the regulatory mechanism of NXPH4 was investigated in colon cancer cells. It was revealed that NXPH4 is also abnormally expressed in CRC cells, and NXPH4 knockdown can significantly inhibit CRC cell proliferation, induce apoptosis and inhibit metastasis and glycolysis.

Next, the regulatory mechanism of NXPH4 in CRC was discussed. The JASPAR database predicted that the promoters of transcription factors FOXK1 and NXPH4 had binding sites. Luciferase and ChIP experiments were also performed to verify the binding ability between FOXK1 and NXPH4. In addition, the present study revealed that FOXK1 expression was significantly elevated in CRC cells. A previous study showed that circAPLP2 interference inhibits tumor growth in CRC, and inhibits *in vitro* glycolysis through the upregulation of microRNA (miR)-485-5p and downregulation of FOXK1 (20). tRF3008A inhibits the progression and metastasis of CRC by destabilizing FOXK1 in an AGO-dependent manner (21). The interaction of FOXK1 and four and a half LIM domains 2 promotes the proliferation, invasion and metastasis of CRC (22). These results indicated that FOXK1 plays an important role as a regulatory factor in the proliferation, metastasis and glycolysis of CRC. In the present study, it was revealed that the overexpression of transcription factor FOXK1 reversed the effect of interfering with NXPH4 on CRC cells.

The present article has some limitations. First of all, only the expression of NXPH4 was downregulated in the current paper, and the overexpression of NXPH4 was not investigated. Only the overexpression of FOXK1 was detected in the current study, and the knockdown of FOXK1 was not investigated. We will further supplement relevant content in future experiments. In addition, another limitation of the present study is that only the HCT116 cell line was used. Due to the amount of data, future experiments will further verify it in other CRC cell lines.

In conclusion, FOXK1-regulated NXPH4 promotes CRC cell proliferation, metastasis and glycolysis. The present study provided a strong theoretical basis for the targeted therapy of CRC and the search for CRC tumor markers.

## Availability of data and materials

The datasets used and/or analyzed during the current study are available from the corresponding author on reasonable request.

## Authors' contributions

YS designed the experiments. QF and WH performed the experiments and wrote the article. QF, WH and YS analyzed the experimental data. QF, WH and YS confirm the authenticity of all the raw data. All the authors have read and approved the final manuscript.

## Ethics approval and consent to participate

Not applicable.

## Patient consent for publication

Not applicable.

## Competing interests

The declare that they have no competing interests.

## References

1. Bray F, Ferlay J, Soerjomataram I, Siegel RL, Torre LA and Jemal A: Global cancer statistics 2018: GLOBOCAN estimates of incidence and mortality worldwide for 36 cancers in 185 countries. CA Cancer J Clin 68: 394-424, 2018.
2. ESMO Guidelines Working Group; Van Cutsem EJD: Advanced colorectal cancer: ESMO clinical recommendations for diagnosis, treatment and follow-up. Ann Oncol 18 (Suppl 2): ii25-ii26, 2007.
3. Kow AWC: Hepatic metastasis from colorectal cancer. J Gastrointest Oncol 10: 1274-1298, 2019.
4. Muller MF, Ibrahim AE and Arends MJ: Molecular pathological classification of colorectal cancer. Virchows Arch 469: 125-134, 2016.
5. Piawah S and Venook AP: Targeted therapy for colorectal cancer metastases: A review of current methods of molecularly targeted therapy and the use of tumor biomarkers in the treatment of metastatic colorectal cancer. Cancer 125: 4139-4147, 2019.
6. Gui Z, Ying X and Liu C: NXPH4 Used as a new prognostic and immunotherapeutic marker for muscle-invasive bladder cancer. J Oncol 2022: 4271409, 2022.
7. Tang Q, Chen YM, Shen MM, Dai W, Liang H, Liu JN and Gao J: Increased expression of NXPH4 correlates with immune cell infiltration and unfavorable prognosis in hepatocellular carcinoma. J Oncol 2022: 5005747, 2022.
8. Zhou L, Rueda M and Alkhateeb A: Classification of breast cancer Nottingham prognostic index using high-dimensional embedding and residual neural network. Cancers (Basel) 14: 934, 2022.

9. Yang Z, Wei B, Qiao A, Yang P, Chen W, Zhen D and Qiu X: A novel EZH2/NXPH4/CDKN2A axis is involved in regulating the proliferation and migration of non-small cell lung cancer cells. Biosci Biotechnol Biochem 86: 340-350, 2022.

10. Li JH, Liu S, Zhou H, Qu LH and Yang JH: starBase v2.0: Decoding miRNA-ceRNA, miRNA-ncRNA and protein-RNA interaction networks from large-scale CLIP-Seq data. Nucleic Acids Res 42 (Database issue): D92-D47, 2014.

11. Lanczky A and Gyorffy B: Web-based survival analysis tool tailored for medical research (KMplot): Development and implementation. J Med Internet Res 23: e27633, 2021.

12. Fornes O, Castro-Mondragon JA, Khan A, van der Lee R, Zhang X, Richmond PA, Modi BP, Correard S, Gheorghe M, Baranašić D, *et al*: JASPAR 2020: Update of the open-access database of transcription factor binding profiles. Nucleic Acids Res 48: D87-D92, 2020.

13. Livak KJ and Schmittgen TD: Analysis of relative gene expression data using real-time quantitative PCR and the 2(-Delta Delta C(T)) method. Methods 25: 402-408, 2001.

14. Arnold M, Sierra MS, Laversanne M, Soerjomataram I, Jemal A and Bray F: Global patterns and trends in colorectal cancer incidence and mortality. Gut 66: 683-691, 2017.

15. Stiksma J, Grootendorst DC and van der Linden PW: CA 19-9 as a marker in addition to CEA to monitor colorectal cancer. Clin Colorectal Cancer 13: 239-244, 2014.

16. Li J, Ma X, Chakravarti D, Shalapour S and DePinho RA: Genetic and biological hallmarks of colorectal cancer. Genes Dev 35: 787-820, 2021.

17. Lech G, Słotwiński R, Słodkowski M and Krasnodębski IW: Colorectal cancer tumour markers and biomarkers: Recent therapeutic advances. World J Gastroenterol 22: 1745-1755, 2016.

18. Eun JW, Jang JW, Yang HD, Kim J, Kim SY, Na MJ, Shin E, Ha JW, Jeon S, Ahn YM, *et al*: Serum proteins, HMMR, NXPH4, PITX1 and THBS4; a panel of biomarkers for early diagnosis of hepatocellular carcinoma. J Clin Med 11: 2128, 2022.

19. Wang D, Zhang P, Liu Z, Xing' Y and Xiao Y: NXPH4 promotes gemcitabine resistance in bladder cancer by enhancing reactive oxygen species and glycolysis activation through modulating NDUFA4L2. Cancers (Basel) 14: 3782, 2022.

20. Liu J, Zhang J, Wang Z, Xi Y, Bai L and Zhang Y: Knockdown of circAPLP2 inhibits progression of colorectal cancer by regulating miR-485-5p/FOXK1 axis. Cancer Biother Radiopharm 36: 737-752, 2021.

21. Han Y, Peng Y, Liu S, Wang X, Cai C, Guo C, Chen Y, Gao L, Huang Q, He M, *et al*: tRF3008A suppresses the progression and metastasis of colorectal cancer by destabilizing FOXK1 in an AGO-dependent manner. J Exp Clin Cancer Res 41: 32, 2022.

22. Wu M, Wang J, Tang W, Zhan X, Li Y, Peng Y, Huang X, Bai Y, Zhao J, Li A, *et al*: FOXK1 interaction with FHL2 promotes proliferation, invasion and metastasis in colorectal cancer. Oncogenesis 5: e271, 2016.